*J. Fluid Mech.* (2012), *vol.* 695, *pp.* 235–256.  
doi:10.1017/jfm.2012.13

# Instability and hydraulics of turbulent stratified shear flows

**Zhiyu Liu[1]†, S. A. Thorpe[2] and W. D. Smyth[3]**

[1] State Key Laboratory of Marine Environmental Science, Xiamen University, Xiamen 361005, China

[2] School of Ocean Sciences, Bangor University, Gwynedd LL59 5EY, UK

[3] College of Oceanic and Atmospheric Sciences, Oregon State University, Corvallis, OR 97331, USA

(Received 31 August 2011; revised 24 October 2011; accepted 26 December 2011;
first published online 20 February 2012)

The Taylor–Goldstein (T–G) equation is extended to include the effects of small-scale turbulence represented by non-uniform vertical and horizontal eddy viscosity and diffusion coefficients. The vertical coefficients of viscosity and diffusion, $A_V$ and $K_V$, respectively, are assumed to be equal and are expressed in terms of the buoyancy frequency of the flow, $N$, and the dissipation rate of turbulent kinetic energy per unit mass, $\varepsilon$, quantities that can be measured in the sea. The horizontal eddy coefficients, $A_H$ and $K_H$, are taken to be proportional to the dimensionally correct form, $\varepsilon^{1/3}l^{4/3}$, found appropriate in the description of horizontal dispersion of a field of passive markers of scale $l$. The extended T–G equation is applied to examine the stability and greatest growth rates in a turbulent shear flow in stratified waters near a sill, that at the entrance to the Clyde Sea in the west of Scotland. Here the main effect of turbulence is a tendency towards stabilizing the flow; the greatest growth rates of small unstable disturbances decrease, and in some cases flows that are unstable in the absence of turbulence are stabilized when its effects are included. It is conjectured that stabilization of a flow by turbulence may lead to a repeating cycle in which a flow with low levels of turbulence becomes unstable, increasing the turbulent dissipation rate and so stabilizing the flow. The collapse of turbulence then leads to a condition in which the flow may again become unstable, the cycle repeating. Two parameters are used to describe the 'marginality' of the observed flows. One is based on the proximity of the minimum flow Richardson number to the critical Richardson number, the other on the change in dissipation rate required to stabilize or destabilize an observed flow. The latter is related to the change needed in the flow Reynolds number to achieve zero growth rate. The unstable flows, typical of the Clyde Sea site, are relatively further from neutral stability in Reynolds number than in Richardson number. The effects of turbulence on the hydraulic state of the flow are assessed by examining the speed and propagation direction of long waves in the Clyde Sea. Results are compared to those obtained using the T–G equation without turbulent viscosity or diffusivity. Turbulence may change the state of a flow from subcritical to supercritical.

**Key words:** mixing and dispersion, stratified flows, turbulent transition

† Email address for correspondence: zyliu@xmu.edu.cn

## 1. Introduction

Our purpose is to examine the effect of turbulence on the stability and hydraulic state of stably stratified shear flows. This relates to the understanding of how mixing takes places in naturally occurring flows, with particular application to the ocean.

The gradient Richardson number is defined as $Ri = N^2/S^2$, where $N(z)$ is the buoyancy frequency and $S$ is the vertical gradient of a horizontal flow. The Miles–Howard theorem (Howard 1961; Miles 1961; Drazin & Reid 1981) states that if the Richardson number in a steady, parallel, horizontal, inviscid and non-diffusive stratified shear flow is everywhere greater than 1/4, the flow is stable to small disturbances of all wavenumbers. A sufficient condition for stability is therefore that the minimum Richardson number, $Ri_{min}$, in the flow exceeds 1/4 as has been explained in mechanical terms by Baines & Mitsudera (1994). A critical Richardson number, $Ri_c$, marks a transition from stable to unstable flow: for $Ri_{min} \leqslant Ri_c$ (which must be $\leqslant 1/4$) there exist small disturbances that grow and the flow is unstable. A flow can be described as being in a state of 'marginal' stability when $Ri_{min} \approx Ri_c$. The growth rates of unstable disturbances of given wavenumber are found by solving the Taylor–Goldstein (T–G) equation (Thorpe 1969; Drazin & Reid 1981).

The Miles–Howard theorem has had an impact on the thinking about naturally occurring flows beyond its strict range of application. In analysing data to determine the state of such flows, it is often – incorrectly – assumed that flows will be unstable if $Ri_{min} < 1/4$, i.e. that $Ri_c = 1/4$. Critical values, $Ri_c$, for example of mean flows measured in the seas of the UK continental shelf, are however often substantially less than 1/4 (e.g. Liu 2010). Flows are rarely parallel or 'unidirectional'; currents usually change in direction as depth increases. It can be shown, however (as in the Appendix), that a steady, inviscid and non-diffusive flow with horizontal components, $U(z)$ and $V(z)$, is stable to small two-dimensional disturbances provided that $Ri = N^2/[(\mathrm{d}U/\mathrm{d}z)^2 + (\mathrm{d}V/\mathrm{d}z)^2]$ exceeds 1/4 everywhere in the flow. (This is a consequence of the fact that only the component of the flow in the horizontal direction of a small disturbance appears in the equations governing its stability.) Several authors have examined the stability of stratified flows in the ocean (e.g. Sun, Smyth & Moum 1998; Liu 2010) and in lakes (e.g. Thorpe & Hall 1977; Thorpe & Ozen 2007; Zika 2008; Thorpe & Liu 2009), but generally set aside any effects of viscosity and diffusion.

Some measures of these effects are, however, available. The T–G equation is extended by Koppel (1964) to include the effects of constant viscosity and diffusivity. Constant *molecular* viscosity and diffusivity may reduce $Ri_c$, tending to make flows more stable, as found for example by Maslowe & Thompson (1971) for a flow with constant $N$ and hyperbolic tangent velocity profile at a Prandtl number, $Pr$, of 0.72, while Gage (1971) shows that, in contrast to the Miles–Howard theorem, flows over a plane boundary with constant $N$, $Pr = 1$ and with no inflection points, e.g. boundary layer flows, are stable to small perturbations provided $Ri_{min} > 0.0554$. (A corollary is that, in a flow with constant $N$ and $Pr = 1$, $Ri_c$ can exceed 0.0554 only if the flow has an inflection point.)

But natural flows are usually turbulent at small scales, turbulence often surviving from earlier strong mixing events possibly caused by its instability or through the breaking of internal waves. Turbulent Reynolds stresses vary in the vertical direction and generally transfer momentum at rates far greater than molecular viscosity, and the variable turbulent buoyancy fluxes transfer buoyancy faster than molecular diffusivity. How great an effect has this residual or 'background' turbulence on the stability of flows?

Smyth, Moum & Nash (2011) is the only paper known to the authors in which small-scale turbulence is taken into account in analysing the growth of unstable disturbances in a measured, naturally occurring flow. Those authors represent turbulence by introducing vertical eddy (or diapycnal) viscosity and diffusivity coefficients set in an *ad hoc* manner to the constant value, $1 \times 10^{-4}$ m$^2$ s$^{-1}$. No study of the stability of an observed flow to small disturbances seems to have been made to assess the effects of turbulence represented by vertical eddy coefficients that vary in depth (selected, for example as in § 3, to accord with observed values of $\varepsilon$), nor has attention been given to the horizontal effects of turbulence on the stability of observed flows.

Our goal is to develop equations and a methodology through which to examine such effects on the stability of a stratified shear flow and also, as described below, on its hydraulic state. These are applied to measurements of a turbulent flow near a sill in the Clyde Sea off the western Scottish coast. When supposed inviscid and non-diffusive, the mean flow is found to be frequently unstable to small disturbances and often in a marginal state (Liu 2010). We shall examine how turbulence may affect $Ri_c$ and hence the marginality of the flow.

The hydraulic state relates to the occurrence of shock waves or hydraulic jumps (Baines 1995) and to mixing, particularly in deep ocean channels (Thorpe 2010) and stratified fjords (e.g. Gregg & Pratt 2010), and is, like its stability to small disturbances, determined by solution of the T–G equation, in this case by seeking solutions for the speed of long waves, found by setting the wavenumber equal to zero. In a stratified shear flow there are generally two wave speeds for each internal wave mode (denoted below by + and − signs before their mode number). Supercritical conditions are those in which no internal waves can travel in one particular direction. This would be the upstream direction in the study of the hydraulics of a uniform flow with a free surface. The meaning of the term 'upstream' is however often lost in stratified shear flows where the flow may reverse its direction through the water column. In subcritical flows long waves can travel in both directions. Bell's (1974) theorem (not to be confused with the quantum mechanical result of the same name) limits and orders the speed of internal waves of different modes. The wave speeds, $c_n$ and $c_{-n}$, of all modes, where $n$ denotes the mode number, lie outside the range of the basic flow, $U_{min} \leqslant U(z) \leqslant U_{max}$, but are ordered within the ranges $U_{min} - N_{max}D/\pi < c_{-1} < c_{-2} < c_{-3} < \cdots < U_{min}$ and $U_{max} < \cdots < c_3 < c_2 < c_1 < U_{max} + N_{max}D/\pi$ determined by the maximum buoyancy frequency, $N_{max}$, and the depth, $D$, of the water column. The wave speeds approach the limits $U_{min}$ and $U_{max}$ as the mode number tends to infinity. (Similar results apply for waves in channels of arbitrary cross-section; Pratt *et al.* 2000.) The theorem, however, is only proved by Bell to be valid when $Ri_{min} \geqslant 1/4$. (At least one example is known in which the speeds of long waves are mode ordered and bounded above by $U_{min}$ even though $Ri_{min} < 1/4$: see Appendix E and figure 4 of Thorpe 2010 when the parameter, $\eta$, defining the flow profile exceeds 2/3 and $8(1-\eta) < Fr < Fr_c$.)

In practice, this condition is not always satisfied. The direction of propagation of long waves in the flow near the Clyde Sea sill allows the flow to be categorised as super- or subcritical, the former applying when waves can only propagate in one direction relative to the sill. We examine the effects of turbulence on the speeds of long waves of different modes, and hence on the flow hydraulics. (Hogg, Winters & Ivey 2001 use Koppel's 1964 extended T–G equation, including the vertical effects of *constant* viscosity and diffusivity, to examine the criticality of an idealised flow through a constriction.)

In § 2 the equations of motion, with the effects of turbulence represented by non-uniform eddy coefficients of viscosity and diffusion, are perturbed around a mean state. Equations are derived that correspond to the T–G equation but extended to include turbulent effects. They are later considered in three separate limits: Limit 1, without viscous, diffusive or turbulent effects; Limit 2, with only the effects of vertical transfers of momentum and mass; and Limit 3, with both vertical and horizontal transfers. We explain in § 3 how values of the vertical and horizontal eddy coefficients are selected in ways that can be determined from data to which the analysis is applied, in particular to the data available in the Clyde Sea (§ 4). These consist of hourly averaged vertical profiles of the horizontal velocity, the buoyancy frequency, $N(z)$, and the rate of dissipation of turbulent kinetic energy per unit mass, $\varepsilon$.

Methods adopted to find critical conditions in which the flow becomes unstable (the critical Richardson numbers, $Ri_c$, of the mean flow and a measure, $\Theta_c$, of the dissipation rate required to stabilize flows) are described in § 5. A range of effects are illustrated by selecting particular hourly periods in the Clyde Sea, and these are presented in § 6 ($Ri_c$ in § 6.1, $\Theta_c$ in § 6.2, and hydraulics in § 6.3). The examples show that growth rates may be reduced, and flow completely stabilised, by the inclusion of turbulent effects; increase in $\varepsilon$ (or decrease in an effective Reynolds number) may stabilize a flow. An example is found in which the hydraulic state of the flow is changed from subcritical to supercritical by turbulence. The results are reviewed, and their implications discussed, in § 7.

## 2. The equations of perturbed flow

The equations of motion are represented as

$$\frac{\mathrm{D}\boldsymbol{u}}{\mathrm{D}t} = -\frac{\boldsymbol{\nabla} p}{\rho_0} + b\boldsymbol{z} + \boldsymbol{\nabla}_H \cdot (A_H \boldsymbol{\nabla}_H \boldsymbol{u}) + \frac{\partial}{\partial z}\left(A_V \frac{\partial \boldsymbol{u}}{\partial z}\right). \tag{2.1}$$

Here $\mathrm{D}/\mathrm{D}t \equiv \partial/\partial t + \boldsymbol{u} \cdot \boldsymbol{\nabla}$, the flow velocity is $\boldsymbol{u} = (U(z,t) + u, V(z,t) + v, w)$, buoyancy is $b = -g(\rho - \rho_0)/\rho_0$, where $g$ is the acceleration due to gravity, the density is $\rho = \Pi(z,t) + \rho'$, and $\rho_0$ is a reference density, $p = P(x,y,z,t) + p'$ is the pressure, $\boldsymbol{\nabla} = (\partial/\partial x, \partial/\partial y, \partial/\partial z)$, $\boldsymbol{\nabla}_H = (\partial/\partial x, \partial/\partial y, 0)$, $\boldsymbol{z} = (0,0,1)$, and $A_H(z,t)$ is the horizontal eddy coefficient of turbulent viscosity (supposed independent of horizontal direction) and $A_V(z,t)$ is the vertical eddy coefficient. The disturbances, $(u,v,w)$ and $b' = -g\rho'/\rho_0$, to the mean flow, $(U,V,0)$ and $\Pi$, and the consequent disturbance to the pressure, $p'$, are taken to be small compared to the mean values. The volume conservation relation is

$$\boldsymbol{\nabla} \cdot \boldsymbol{u} = 0, \tag{2.2}$$

and the equation for continuity of density of the fluid, supposed incompressible, is

$$\frac{\mathrm{D}b}{\mathrm{D}t} = \boldsymbol{\nabla}_H \cdot (K_H \boldsymbol{\nabla}_H b) + \frac{\partial}{\partial z}\left(K_V \frac{\partial b}{\partial z}\right), \tag{2.3}$$

where $K_H(z,t)$ and $K_V(z,t)$ are the horizontal (again supposed isotropic) and vertical eddy coefficients of turbulent diffusivity, respectively. Equations (2.1)–(2.3) are standard equations adopted to represent turbulence, in particular its transfers of momentum and mass, but they involve assumptions about the homogeneity and nature of turbulence (see e.g. Kantha & Clayson 2000). For example, by taking a single

horizontal eddy coefficient different from the vertical coefficient it is supposed that, because of stratification, the vertical effects of turbulence differ from the horizontal but that the effects are isotropic in the horizontal direction. The selected forms of the eddy coefficients are described in § 3. In using these equations to describe the effects of a spatially periodic perturbation to a mean flow, it is implicit that there is a scale separation between the small-scale three-dimensional turbulence and the perturbation. We shall find in § 6.1 that, for the Clyde Sea data, the vertical scale of the fastest growing disturbances exceeds the Ozmidov scale, $L_{Oz} = \varepsilon^{1/2}/N^{3/2}$, representing the largest overturning turbulent eddies. There are, however, no observations available from which to estimate the horizontal scale of turbulent eddies and to confirm that they are substantially less than the horizontal scale (typically ∼20 m; § 6) of the fastest growing disturbances.

The equations for the mean flow are

$$\frac{\partial U}{\partial t} = -\frac{1}{\rho_0}\frac{\partial P}{\partial x} + \frac{\mathrm{d}A_V}{\mathrm{d}z}\frac{\partial U}{\partial z} + A_V\frac{\partial^2 U}{\partial z^2}, \tag{2.4}$$

$$\frac{\partial V}{\partial t} = -\frac{1}{\rho_0}\frac{\partial P}{\partial y} + \frac{\mathrm{d}A_V}{\mathrm{d}z}\frac{\partial V}{\partial z} + A_V\frac{\partial^2 V}{\partial z^2}, \tag{2.5}$$

$$0 = -\frac{\partial P}{\partial z} - \rho_0 B, \tag{2.6}$$

and

$$\frac{\partial B}{\partial t} = \frac{\mathrm{d}K_V}{\mathrm{d}z}\frac{\partial B}{\partial z} + K_V\frac{\partial^2 B}{\partial z^2}, \tag{2.7}$$

where the mean buoyancy $B = -g(\Pi - \rho_0)/\rho_0$. As noted by Smyth *et al.* (2011), the mean flow, $U$ and $V$, and density, $\Pi$, are therefore steady if the $x$- and $y$-pressure gradients balance the action of turbulent viscosity on the mean flow, or, if both are negligible, if the vertical pressure gradient is in hydrostatic balance, and if the action of vertical turbulent diffusion is negligible, at least within the time scale of the growth of instabilities. Assuming these conditions are valid, we henceforth assume that the mean flow is steady so that $U$, $V$, $\Pi$ (or $B$), $A_H$, $A_V$, $K_H$ and $K_V$, are functions only of $z$. Omitted from the present consideration is any modification of turbulence that results from the presence of the disturbance to the mean flow; the eddy coefficients are supposed independent of the amplitude of the perturbation, at least to first-order. Any changes to turbulence, represented here by the eddy coefficients, caused by its straining and shearing by the spatially periodic and temporally growing, but small, disturbances are disregarded. This subject demands further study beyond our present scope.

Linearized or first-order equations for the disturbances, $u$, $v$, $w$ and $b'$, can now be found. Henceforth, without loss of generality, designating $U(z)$ as the mean flow velocity component in the direction of a two-dimensional disturbance in the $x$-direction (and with no variation in $y$ so all the terms involving $y$-derivatives are now zero), the $x$- and $z$-equations of motion reduce to

$$\frac{\partial u}{\partial t} + U\frac{\partial u}{\partial x} + w\frac{\mathrm{d}U}{\mathrm{d}z} = -\frac{1}{\rho_0}\frac{\partial p'}{\partial x} + A_H\frac{\partial^2 u}{\partial x^2} + A_V\frac{\partial^2 u}{\partial z^2} + \frac{\mathrm{d}A_V}{\mathrm{d}z}\frac{\partial u}{\partial z}, \tag{2.8}$$

and

$$\frac{\partial w}{\partial t} + U\frac{\partial w}{\partial x} = -\frac{1}{\rho_0}\frac{\partial p'}{\partial z} + b' + A_H\frac{\partial^2 w}{\partial x^2} + A_V\frac{\partial^2 w}{\partial z^2} + \frac{\mathrm{d}A_V}{\mathrm{d}z}\frac{\partial w}{\partial z}, \tag{2.9}$$

with volume conservation

$$\frac{\partial u}{\partial x} + \frac{\partial w}{\partial z} = 0, \tag{2.10}$$

and density conservation

$$\frac{\partial b'}{\partial t} + U\frac{\partial b'}{\partial x} + w\frac{\mathrm{d}B}{\mathrm{d}z} = K_H\frac{\partial^2 b'}{\partial x^2} + Kv\frac{\partial^2 b'}{\partial z^2} + \frac{\mathrm{d}K_V}{\mathrm{d}z}\frac{\partial b'}{\partial z}. \tag{2.11}$$

These are independent of the components, $V$ and $v$, of the mean flow and disturbance in direction $y$.

Eliminating $p'$ by subtracting the $x$-derivative of (2.9) from the $z$-derivative of (2.8), and introducing a stream function $\psi$, where $u = \partial\psi/\partial z$ and $w = -\partial\psi/\partial x$, so satisfying (2.10), we obtain

$$\begin{aligned}\left(\frac{\partial}{\partial t} + U\frac{\partial}{\partial x}\right)\nabla^2\psi - \frac{\mathrm{d}^2 U}{\mathrm{d}z^2}\frac{\partial\psi}{\partial x} \\ = -\frac{\partial b'}{\partial x} + A_H\frac{\partial^2}{\partial x^2}\nabla^2\psi + \frac{\mathrm{d}A_H}{\mathrm{d}z}\frac{\partial^3\psi}{\partial z\partial x^2} + \frac{\mathrm{d}A_V}{\mathrm{d}z}\left(\frac{\partial^2}{\partial x^2} + 2\frac{\partial^2}{\partial z^2}\right) \\ \times\frac{\partial\psi}{\partial z} + A_V\frac{\partial^2}{\partial z^2}\nabla^2\psi + \frac{\mathrm{d}^2 A_V}{\mathrm{d}z^2}\frac{\partial^2\psi}{\partial z^2},\end{aligned} \tag{2.12}$$

while, noting that $N^2 = \mathrm{d}B/\mathrm{d}z$, (2.11) becomes

$$\left(\frac{\partial}{\partial t} + U\frac{\partial}{\partial x}\right)b' - N^2\frac{\partial\psi}{\partial x} = K_H\frac{\partial^2 b'}{\partial x^2} + K_V\frac{\partial^2 b'}{\partial z^2} + \frac{\mathrm{d}K_V}{\mathrm{d}z}\frac{\partial b'}{\partial z}. \tag{2.13}$$

Expressing the perturbed terms as $\psi = \phi(z)\exp(\mathrm{i}kx + \sigma t)$ and $b' = \beta(z)\exp(\mathrm{i}kx + \sigma t)$ where $\sigma = \sigma_r + \mathrm{i}\sigma_i$ is the complex frequency and $k$ is the wavenumber of the disturbance, and writing the vertical component of velocity $w = -\partial\psi/\partial x = -\mathrm{i}k\phi\exp(\mathrm{i}kx + \sigma t) = \hat{w}\exp(\mathrm{i}kx + \sigma t)$ so that $\phi = \mathrm{i}\hat{w}/k$, (2.12) and (2.13) reduce to

$$\sigma\left(\frac{\mathrm{d}^2}{\mathrm{d}z^2} - k^2\right)\hat{w} = \left[-\mathrm{i}kU\left(\frac{\mathrm{d}^2}{\mathrm{d}z^2} - k^2\right) + \mathrm{i}k\frac{\mathrm{d}^2 U}{\mathrm{d}z^2} + F_w\right]\hat{w} - k^2\beta, \tag{2.14}$$

and

$$\sigma\beta = -N^2\hat{w} + [-\mathrm{i}kU + F_\beta]\beta, \tag{2.15}$$

since $N^2 = \mathrm{d}B/\mathrm{d}z$, and where the operators, $F_w$ and $F_\beta$, involving the turbulent eddy coefficients, are functions of $z$, and are given by

$$F_w = \frac{\mathrm{d}^2}{\mathrm{d}z^2}\left(A_V\frac{\mathrm{d}^2}{\mathrm{d}z^2}\right) - k^2\frac{\mathrm{d}}{\mathrm{d}z}\left[(A_H + A_V)\frac{\mathrm{d}}{\mathrm{d}z}\right] + k^4 A_H, \tag{2.16}$$

$$F_\beta = \frac{\mathrm{d}}{\mathrm{d}z}\left(K_V\frac{\mathrm{d}}{\mathrm{d}z}\right) - k^2 K_H. \tag{2.17}$$

Equations (2.14) and (2.15), with boundary conditions $\hat{w} = 0$ and $\beta = 0$ at the lower and upper boundaries, are in a form that can be solved by the matrix method, as in

Smyth *et al.* (2011); the stability of the mean flow for disturbance wavenumber, $k$, can be determined in the usual way by examination of the eigenvalues, $c = c_r + \mathrm{i}c_i = \mathrm{i}\sigma/k$.

If the terms involving $F_w$ and $F_\beta$ are set to zero, or equivalently if $A_V$, $K_V$, $A_H$ and $K_H$ are set to zero, elimination of $\beta$ between the two equations reduces them to a single equation for $\phi$, the conventional T–G equation from which, for a unidirectional flow, the Miles–Howard theorem is derived. We shall refer to this as 'Limit 1'. Two other limiting cases are considered to gain insight into the effects of turbulence on the stability of the flow. In 'Limit 2' the coefficients $A_H$ and $K_H$ are set equal to zero; only the effects of *vertical* transfers of momentum and mass by turbulence represented by the terms including $A_V$ and $K_V$ are included. In 'Limit 3', we include both *vertical* and *horizontal* effects.

## 3. The turbulent eddy coefficients

### 3.1. *The vertical eddy coefficients*

To make the solution of (2.14) and (2.15) of practical value in interpreting the data from the Clyde Sea, expressions for the eddy coefficients are required in terms of quantities, e.g. $N$, $U$ and $\varepsilon$, that can be measured. The conventional relations derived from the steady-state energy balance in which the rate of dissipation of turbulent kinetic energy is equal to the rate of production by the mean flow plus the buoyancy flux, lead to

$$K_V = \frac{\Gamma\varepsilon}{N^2}, \tag{3.1}$$

where $\varepsilon$ is the rate of loss of turbulent kinetic energy per unit mass and $\Gamma$ is an efficiency parameter (Osborn 1980). Selecting the commonly used value $\Gamma = 0.2$, and since the turbulent Prandtl number, $Pr_t = A_V/K_V \approx 1$ (Shih *et al.* 2005) over much of the range of the observed values of $I = \varepsilon/\nu N^2$, we have

$$K_V = A_V = \frac{0.2\varepsilon}{N^2}. \tag{3.2}$$

According to Shih *et al.* (2005), $\Gamma \approx 0.2$ is valid in the range $7 < I = \varepsilon/\nu N^2 < 100$, but may possibly overestimate $K_V$ outside this range. The uncertainty in the value of $\Gamma$ is described by, e.g., Smyth, Moum & Caldwell (2001). Alternatively we might adopt the relation between the flux Richardson number, $R_f$, and the gradient Richardson number: $R_f/Ri = K_V/A_V = q(1 - R_f/R_{fc})/(1 - R_f)^2$, given by Turner (1973, his equation 5.2.23) with constant $q \approx 1.4$. This equation has a best fit to laboratory data when $R_{fc} \approx 0.15$, and provides the means of finding $R_f$ from measured values of $Ri$. It follows that $A_V = [Ri/(1 - R_f)]\varepsilon/N^2$, but this, without some further relationship, leaves the value of $R_f$ unspecified by the available data. Zilitinkevich *et al.* (2008) review meteorological, laboratory and numerical data showing $Pr_t \approx 0.8 + 5Ri$, with an uncertainty of $\sim\pm 0.4$, when $Ri < 1$. A further means of deriving scale-dependent vertical (and horizontal) eddy coefficients in terms of $L_{Oz}$ and $Ri$ based on the use of Langevin equations is described by Galperin, Sukoriansky & Anderson (2007). For simplicity we use (3.2).

### 3.2. *The horizontal eddy coefficients*

There appear to be no accepted equations for $A_H$ and $K_H$ in parametric forms expressed in terms of commonly measurable quantities, and we have therefore resorted to devising plausible formulations. It is assumed that the horizontal eddy coefficients

of turbulent viscosity and diffusivity can be expressed as the dimensionally correct forms

$$A_H = c_A \varepsilon^{1/3} l^{4/3} \tag{3.3a}$$

and

$$K_H = c_K \varepsilon^{1/3} l^{4/3}, \tag{3.3b}$$

respectively, where $l$ is the horizontal scale at which turbulent viscosity or diffusivity are acting (taken as the horizontal wavelength, $2\pi/k$, of the disturbance, typically $\sim$20 m, in our subsequent analysis), and $c_A$ and $c_K$ are non-dimensional constants.

The forms (3.3) are chosen as being consistent with the variation of diffusivity of patches of dye in the upper ocean with horizontal scale, $l$, found by Okubo (1971). Okubo plots the logarithm of a dispersion coefficient, $K_D$, against that of $l$, showing that the data fit lines with 4/3 slopes (so that $K_D \propto l^{4/3}$) over certain limited ranges of horizontal length scale, the lowest being from $\sim$20 m (the smallest for which measurements were available) to $\sim$1 km. The 4/3 power law for dispersion is consistent with that proposed empirically by Richardson. (Ollitrault, Gabillet & De Verdiere 2005, review the evidence for a 4/3 power law and refer to the possibility of a $l^2$ law at scales less than the internal Rossby radius, but provide no compelling observational evidence for the higher power law at these scales. Lacking convincing evidence to the contrary we therefore proceed to use the 4/3 law whilst noting the need for further observational evidence. Ashford 1985 quotes the following from Richardson 1952: 'The atmospheric observations could have been fitted passably by any index between 1.2 and 1.5. The 4/3 was chosen partly as a rough mean, and partly because it simplifies some integrals.') Okubo's data are therefore consistent with

$$K_D = C \varepsilon^{1/3} l^{4/3}, \tag{3.4}$$

with a non-dimensional constant, $C$, provided that $\varepsilon$ remains constant throughout each of the limited range of length scales. The relation (3.4) fits data in a series of ranges of larger and larger length scales with successively smaller constant values of $\varepsilon$ in each range. This suggests that there is an input of energy flux at the upper end of each range of scales, one being at $\sim$1 km, enhancing the flux of energy through the turbulent spectrum towards eventual dissipation at scales comparable to the Kolmogorov scale. Okubo's formulation of $K_D$ does not account for the spatial and temporal variations in the variety of processes that may affect dispersion but it does provide a rough measure of dispersion in many different parts of the ocean (Thorpe 2005), including that of dye released by Sundermeyer & Ledwell (2001) into the thermocline over the New England continental shelf where the water depth is $\sim$70 m, comparable to the 58 m depth in the Clyde Sea measurement area. (Although the non-dimensional parameter $f/N$, where $f$ is the Coriolis parameter, may appear in the formulation of $K_D$ on the New England shelf at scales of 1–10 km as found by Sundermeyer *et al.* 2005, the effect of the Earth's rotation is unlikely to have an effect at the present smaller scales of interest.)

Although horizontal turbulent viscosity, the horizontal turbulent diffusion of density and the horizontal turbulent dispersion of dye are different entities, each depends on the properties of the horizontal field of turbulent eddies. The scaling of the turbulent dispersion coefficient on $\varepsilon$ and $l$ alone in (3.4) suggests (but does not prove) that these two measures may also apply for turbulent viscosity and diffusion, providing the only dimensional quantities through which the eddy coefficients are expressed, and hence constraining their forms to those selected in (3.3). It is implicit in the formulation that

the 'horizontal' density dispersion occurs mainly on isopycnal surfaces and not across them; a criticism of (3.3) is that the selected forms do not account explicitly for the buoyancy frequency, shear or Richardson number at the level of interest.

In the absence of information or empirical data to the contrary, we therefore adopt the forms defined in (3.3) for scales, $l$, of ~20 m. (In later taking $l = 2\pi/k$, where $k$ is the horizontal wavenumber of the two-dimensional disturbance, we do not intend to imply that the small disturbances are those that lead to horizontal turbulent viscosity or diffusion at this scale, although they may affect them – a disregarded effect, see § 2 – but simply that the scale-dependent coefficients have the values assigned when the scales under consideration are equal to the wavelength of the disturbances.) Ledwell, Watson & Law (1998) note that the vertical coefficients of diffusion of density measured by free-fall microstructure probes agree reasonably well with the vertical coefficients of the dispersion of dye in the North Atlantic, and we shall suppose that like their vertical counterparts, the horizontal coefficients are equal, i.e. that $K_H = K_D$.

In the range of horizontal scales from ~20 m to 1 km Okubo's (1971) data are fitted by

$$K_D = (9.3 \pm 1.4) \times 10^{-5} l^{4/3}, \tag{3.5}$$

where the diffusion coefficient, $K_D$, is measured in $m^2\ s^{-1}$ and $l$ in m. Using (3.3) and the observed mean value of $\varepsilon$ in the Clyde Sea of $\sim(4.2 \pm 1.8) \times 10^{-8}$ W $kg^{-1}$ (§ 5), putting $K_H = K_D$ we find $C = c_K = (2.9 \pm 0.8) \times 10^{-2}$. The vertical and horizontal diffusion coefficients are equal at a scale $l_*$ where $K_V = K_H$. Equality occurs at $l_* = L_{Oz}(\Gamma/c_K)^{3/4}$, where $L_{Oz} = \varepsilon^{1/2}/N^{3/2}$ is the Ozmidov length scale. (The vertical and horizontal eddy diffusion coefficients are equal at a horizontal scale, $l_*$, of $\sim 4L_{Oz}$. This appears much too large because isotropy is not expected at scales exceeding $L_{Oz}$. This is discussed further in § 7.) If we assume that the horizontal and vertical viscous transfer coefficients are also equal at this scale, so that $A_V = A_H$ at $l = l_*$, then $c_A = c_K$. In summary, we shall take

$$K_H = A_H = (2.9 \pm 0.8) \times 10^{-2} \varepsilon^{1/3} l^{4/3}. \tag{3.6}$$

## 4. The observations in the Clyde Sea

The site of the measurements used to examine the effect of turbulence in the solutions of (2.14) and (2.15) is in a mean water depth of 58 m to at a distance of approximately 12 km from the 40 m deep crest of a broad sill at the entrance to the Clyde Sea. The flow is strongly affected by $M_2$ baroclinic tides generated at or near the sill, and its direction changes with depth. The crest of the sill is orientated in a southeasterly direction; $\alpha \approx 50°$ represents the direction of internal tidal wave propagation into the Clyde Sea away from the sill. Data consist of vertical profiles of the horizontal velocity from an acoustic Doppler current profiler (ADCP), together with measurements from free-fall fast light yo-yo (FLY) microstructure probes of $N(z)$ and the rate of dissipation of turbulent kinetic energy per unit mass, $\varepsilon$. Temporally averaged data obtained over 12–18 min are available from 24 sequential hourly periods designated, as in Liu (2010), as Hr 0 to Hr 24 (except that no data are available for Hr 20). Analysis is confined to the flow in the mid-water pycnocline, thus excluding the turbulent boundary layer adjoining the seabed. The mid-water flow is generally turbulent with a mean value of $\varepsilon$ of $\sim(4.2 \pm 1.8) \times 10^{-8}$ W $kg^{-1}$.

## 5. Critical conditions: $Ri_c$ and $\Theta_c$

The analysis follows that of Liu (2010) who examines the stability of the hourly flow in the Clyde Sea but only when the flow is supposed to be inviscid and non-diffusive, as in Limit 1. Solutions of (2.14) and (2.15) are found for a given real wavenumber, $k$, and the growth rate, $\sigma_r$ (or $kc_i$), is calculated as a function of the direction, $\alpha$, relative to the north of a small disturbance. Rotating axes, the mean horizontal flow, $U(z)$, in direction $\alpha$ becomes $U_E \sin\alpha + U_N \cos\alpha$, where the observed hourly averaged flow components in the east and north directions are $U_E(z)$ and $U_N(z)$, respectively. The maximum growth rate as $\alpha$ is varied, and the corresponding eigenfunction, $\hat{w}$, is found as in Liu (2010). The variation of the maximum growth rate determined as a function of $k$, and the value of $k$ at which the growth rate is greatest, $(kc_i)_{max}$, can be found, provided the flow is unstable.

The size of the greatest growth rate, $(kc_i)_{max}$, provides useful insight into the state of the flow. Further information is given by determining a critical Richardson number, $Ri_c$. How much must the speed of an unstable flow be reduced before it becomes stable? To investigate this, following Thorpe & Liu (2009) and Liu (2010), the mean flow is scaled by a factor $(1 + \Phi)$, and $\Phi$ is decreased in small steps when the flow is unstable (or increased for stable flows) until, at a value $\Phi = \Phi_c$, the greatest growth rate becomes zero. (This procedure is strictly invalid because of the violation of the assumption that the mean flow described by (2.4) and (2.7) has a growth rate that is relatively small compared to that of the disturbances.) The buoyancy frequency is maintained at its original value, $N(z)$. The minimum Richardson number in the corresponding scaled flow is then equal to $Ri_c$:

$$Ri_c = \frac{Ri_{min}}{(1 + \Phi_c)^2}, \tag{5.1}$$

where $Ri_{min}$ is defined as $\min\{N^2/[(\mathrm{d}U_E/\mathrm{d}z)^2 + (\mathrm{d}U_N/\mathrm{d}z)^2]\}$, as in the Appendix.

Values of the eddy coefficients are required, however, when finding the growth rates in flows scaled with $(1 + \Phi)$. These, given by (3.2) and (3.6), depend on $\varepsilon$, and it is not known how this may change as the mean flow is varied. We adopted two alternatives: first to keep $\varepsilon$ unchanged as $\Phi$ varies, and second to allow $\varepsilon$ to vary as $(1 + \Phi)^3$, having in mind a scaling of $\varepsilon$ proportional to (velocity)$^3$ length$^{-1}$, as in Taylor's inertial scaling (Taylor 1935). The results are found to be relatively insensitive to the selection of the two alternatives, typical variations in $Ri_c$ between the two cases being less than 10 %, and for simplicity in the presented results (e.g. table 1) $\varepsilon$ was kept unchanged. As it later becomes evident (§ 6.2), larger changes in $\varepsilon$ than result from multiplication by $(1 + \Phi)^3$ (typically less than ~4) are required to cause much variation in the growth rates of small disturbances.

Rather than scaling either the mean flow (or possibly the buoyancy frequency) to determine the critical $Ri$, an alternative procedure to obtain insight into the state of the flow is to scale the observed values of $\varepsilon$ by a factor $\Theta$. As in the laminar case with viscosity and molecular diffusion studied by Maslowe & Thompson (1971), the general effect of turbulence (momentum and mass transport) is to reduce the maximum growth rates (§ 6.1). The value of $\Theta = \Theta_c$ at which $(kc_i)_{max}$ becomes equal to zero for flows that are unstable in Limit 1 therefore provides a measure of how much the dissipation rate may have to be increased to stabilize the flow with no variation in $Ri$; alternatively how much greater a flux of energy into the flow field must be supplied with no change to $Ri$, and in a form that will contribute to and be dissipated by turbulence, before the flow becomes stable. Since when keeping the $S$ or

| Hr | $Ri_{min}$ | $(kc_i)_{max}$ $(\times 10^{-3}\ \mathrm{s}^{-1})$ | | | $\Phi_c$ $(\times 10^{-1})$ | | | $Ri_c$ | | | $\Theta_c$ | |
|---|---|---|---|---|---|---|---|---|---|---|---|---|
| | | Limit 1 | Limit 2 | Limit 3 | Limit 1 | Limit 2 | Limit 3 | Limit 1 | Limit 2 | Limit 3 | Limit 2 | Limit 3 |
| 16 | 0.065 | 3.95 | 3.77 | 3.04 | −4.18 | −3.87 | −3.12 | 0.192 | 0.173 | 0.137 | 39.8 | 11.8 |
| 10 | 0.065 | 0.40 | 0.33 | 0 | −0.23 | −0.19 | 0.07 | 0.068 | 0.068 | 0.064 | 13.8 | — |
| 14 | 0.044 | 0 | 0 | 0 | 1.69 | 1.99 | 2.56 | 0.032 | 0.031 | 0.028 | — | — |

TABLE 1. Three examples of the values of $\min\{N^2/[(\mathrm{d}U_E/\mathrm{d}z)^2 + (\mathrm{d}U_N/\mathrm{d}z)^2]\}$ (see the Appendix), $(kc_i)_{max}$, $\Phi_c$, $Ri_c$ and $\Theta_c$ obtained from averaged hourly data in the Clyde Sea, interpolated onto a 0.2 m vertical grid, in the three limits. The eddy coefficients are zero in Limit 1. The vertical eddy coefficients are taken into account in Limit 2, and both vertical and horizontal coefficients are included in Limit 3. The flows are unstable in all three limits at Hr 16 ($Ri_{min} < Ri_c$ and $(kc_i)_{max} > 0$). At Hr 10 flow is unstable in Limits 1 and 2, but stabilized by the addition of horizontal effects at Limit 3. Hr 14 is stable at all three limits. The uncertainty in the values of $Ri_{min}$ estimated from the available data is ∼0.03. The uncertainty in $Ri_c$ derived from interpolation to find $\Phi_c$ when $(kc_i)_{max} = 0$ (accepting the validity of the data) is ∼0.02, and that in $\Theta_c$ is ∼10 %.

velocity profiles constant, the 'vertical' Reynolds number of the flow, $Re_V$, is inversely proportional to $A_V = 0.2\varepsilon/N^2$ and the 'horizontal' Reynolds number, $Re_H$, is inversely proportional to $A_H = (2.9 \pm 0.8) \times 10^{-2}\varepsilon^{1/3}l^{4/3}$ (with appropriate averaging over the fluid depth) variation of $\varepsilon$ is equivalent to a variation of the flow Reynolds numbers, an increase in $\varepsilon$ corresponding to a decrease in $Re_V$. (Variation in $Re_H$ depends on how the wavelength $l$ changes with $\varepsilon$.)

To summarize: values of $\Phi_c$ when $\varepsilon$ is unchanged provide a measure of the proximity of a flow to a critical Richardson number when the flow Reynolds number is held constant, while $\Theta_c$ gives a measure of relation of the flow's Reynolds number to a critical Reynolds number when the Richardson number in the flow is held constant. Both $\Phi_c$ and $\Theta_c$ provide measures of the marginality of the flow.

## 6. Application and results

### 6.1. *Flow stability: $Ri_c$*

Over the 24 hourly periods analysed, the average $Ri_{min}$ (derived as in the Appendix) is 0.087. All but 6 of the hourly periods are unstable with $(kc_i)_{max} > 0$, and $Ri_{min} < Ri_c$ in Limit 1 (with eddy coefficients set to zero). The effect of representing turbulence through eddy viscosity and diffusivity coefficients in the equations of motion is a tendency to stabilize the flow: adding the vertical coefficients (Limit 2) reduces the maximum growth rate of unstable modes, $(kc_i)_{max}$, by an average of 4.9 %, increases the mean $\Phi_c$ by about 5.7 % from −0.335 to −0.316, and reduces the critical Richardson number, $Ri_c$, from 0.140 in Limit 1 to 0.132, a reduction of 5.5 %. The direction of the fastest growing disturbances is found to be the same in Limit 2 (and in Limit 3) as it is in Limit 1. This direction does not coincide with that of the maximum shear or smallest Richardson number based on the component of shear in the disturbance direction, $\mathrm{d}U/\mathrm{d}z$, as in the Appendix, but (for the data examined) the difference in the directions is generally less than 45°.

The average wavelength of the fastest growing disturbances, $\lambda_c$, changes from 31.3 m in Limit 1 to 30.8 m in Limit 2. For Limit 3 the maximum growth rate, $(kc_i)_{max}$, is reduced from the Limit 1 values by an average of 19.0 %, and the mean $\Phi_c$ is −0.259, an increase from Limit 1 of 22.7 % and a closer approach to flow marginality at $\Phi_c = 0$. The mean critical Richardson number, $Ri_c$, is 0.117, a reduction of 16.2 % from Limit 1, and $\lambda_c$ becomes 32.1 m.

Three hourly periods for which data are shown in figures 1 and 2 are selected to illustrate how stability varies in the three limits. In the first example, Hr 16, the flow is unstable (with $Ri_{min} < Ri_c$ and $(kc_i)_{max} > 0$) in all three limits. The flow in the second example, Hr 10, is however unstable in Limits 1 and 2, but is stabilized in Limit 3, and in the final example, Hr 14, the flow is stable in all limits. The velocity component in direction 050, $U_{50}$, used in § 6.3, $N$, $S = [(\mathrm{d}U_E/\mathrm{d}z)^2 + (\mathrm{d}U_N/\mathrm{d}z)^2]^{1/2}$ where $U_E$ and $U_N$ are the east and north components of velocity, together with $\log_{10}\varepsilon$, in the three examples are shown in figure 1. There is no evident correlation of $\varepsilon$ with the other variables. Figure 2 shows the derived profiles of $\log_{10} Ri(=\log_{10}(N^2/S^2))$, $\log_{10} I(=\log_{10}(\varepsilon/\nu N^2))$, $\log_{10} L_{Oz}$, $\log_{10} A_V = \log_{10} K_V$ and $\log_{10} A_H = \log_{10} K_H$. In each example $Ri_{min}$ is less than 1/4 (see table 1). The value of $l$ used to determine $A_H = K_H$ from (3.6) at Hr 16 is that of the maximum growth rate in Limit 3 (see figure 3*a*), but in Hrs 10 and 14, stable in Limit 3, the values of $l$ used are those determined by modifying the velocity profiles by increasing $\Phi$ until the flows became unstable; $l = 17.5$, 28.0 and 30.5 m, in Hrs 16, 10 and 14, respectively. Values of $I = \varepsilon/\nu N^2$

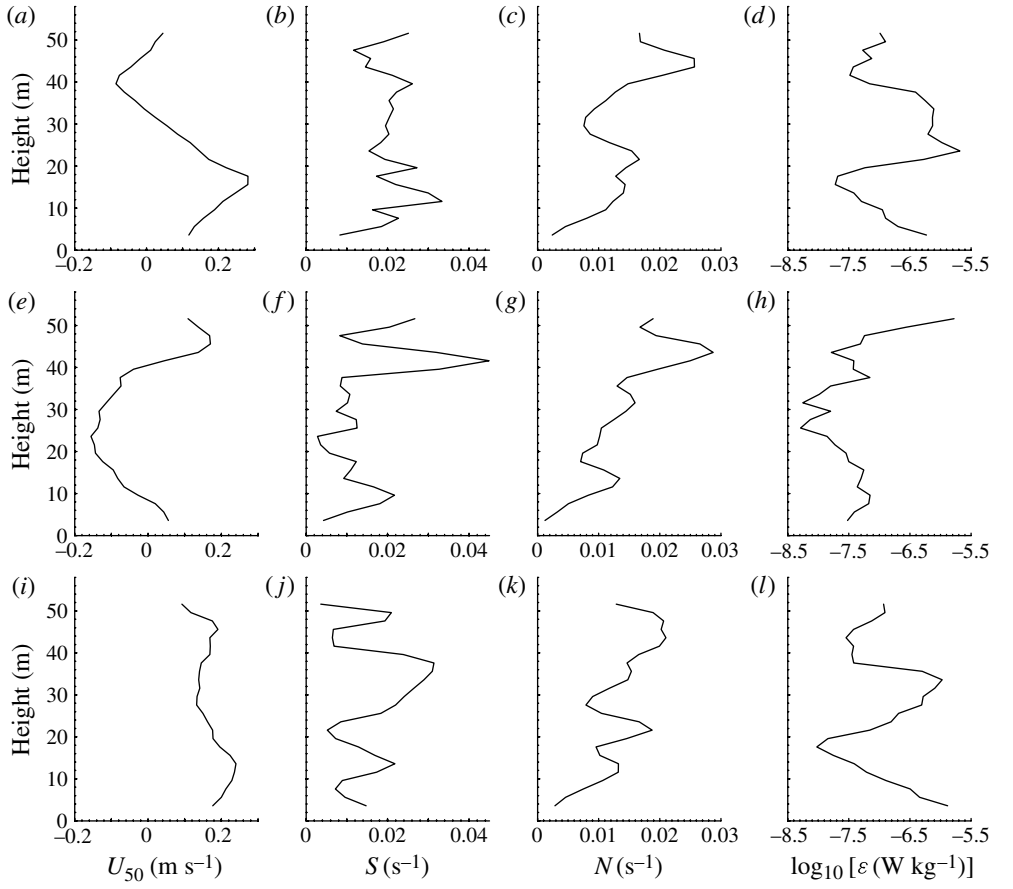


FIGURE 1. The measured profiles of (left to right) the velocity component $U_{50}$ in direction 050° as in § 6.3, $N$, $S = [(\mathrm{d}U_E/\mathrm{d}z)^2 + (\mathrm{d}U_N/\mathrm{d}z)^2]^{1/2}$ where $U_E$ and $U_N$ are the east and north components of velocity, and $\log_{10}\varepsilon$ in the flows at (*a–d*) Hr 16, (*e–h*) Hr 10, and (*i–l*) Hr 14, all plotted versus height above the seabed.

generally exceed 200, indicating that turbulence is commonly isotropic (Gargett, Osborn & Nasmyth 1984). The horizontal eddy coefficients exceed the vertical.

The growth rates, $kc_i$, of the most unstable mode in the three limits are plotted in figure 3 as functions of $kD$, where $D = 58$ m is the water depth. The wavelengths of the fastest growing disturbances are ∼16.8 m in Hr 16 and 27.7 m in Hr 10, and do not vary significantly even though the modal structure of the disturbances changes, as shown in figure 4. The vertical scale of the most unstable modes is ∼8 m, substantially greater than the size, typically <1 m, of $L_{Oz}$ (figure 2).

### 6.2. *Flow stability: $\Theta_c$, varying $\varepsilon$*

Values of $(kc_i)_{max}$ are found with $\varepsilon$ scaled by a factor $\Theta$ in cases in which the flow is unstable in Limit 1. Linear interpolation gives the value of $\Theta = \Theta_c$ at which $(kc_i)_{max}$ becomes equal to zero. The mean value of $\Theta_c$ is 65.5 in Limit 2, but with values ranging from ∼13.8 (in Hr 10) to 235.2: at least one order of magnitude increase in the rate of dissipation observed in the unstable flow is required to stabilize it. A change in $\varepsilon$ by a factor of 65.5 implies that, keeping the velocity and buoyancy

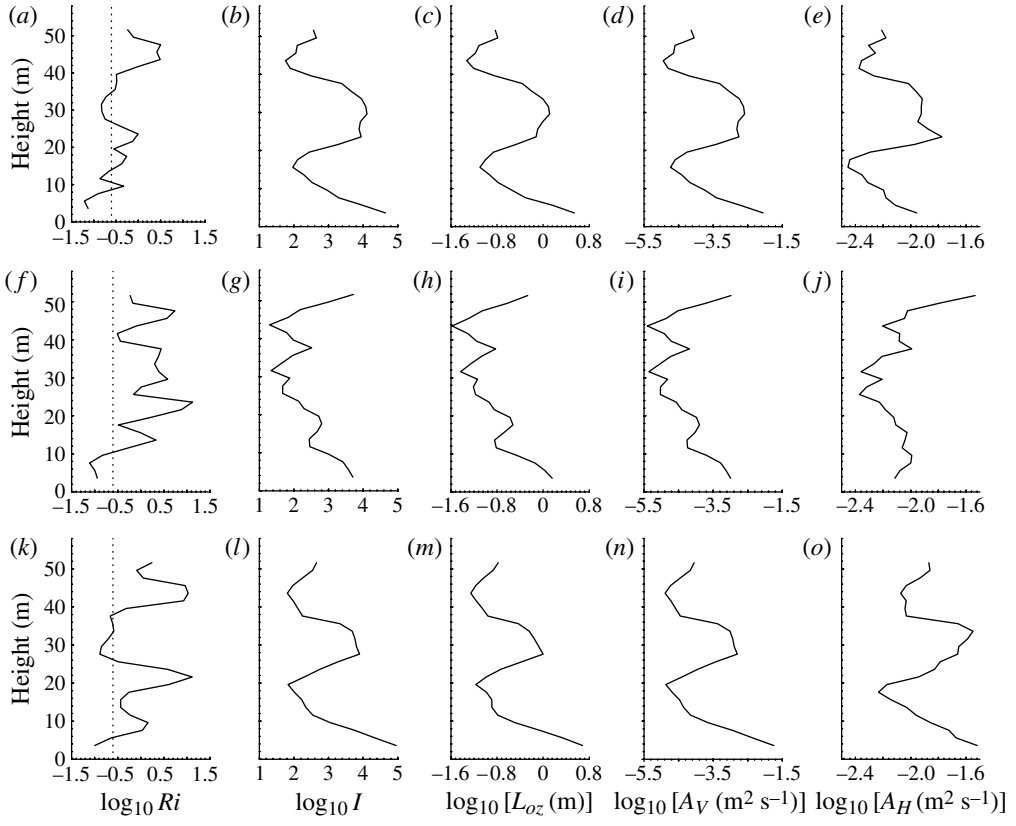


FIGURE 2. Profiles of $\log_{10} Ri = \log_{10}(N^2/S^2)$ (the dotted line marks $Ri = 1/4$), $\log_{10} I = \log_{10}(\varepsilon/\nu N^2)$, $\log_{10} L_{Oz}$, $\log_{10} A_V = \log_{10} K_V$ and $\log_{10} A_H = \log_{10} K_H$ in the flows in Limit 3, at (*a–e*) Hr 16, (*f–j*) Hr 10 and (*k–o*) Hr 14, all plotted versus height above the seabed. (Hrs 10 and 14 are stable in Limit 3. The value of $l$ used in (3.6) to derive $A_H = K_H$ is that determined by modifying the velocity profiles by increasing until the flows became unstable and adopting the value of l for the maximum growth rate.)

profiles constant, the 'vertical' Reynolds number of the flow, $Re_V$, must be reduced by a multiplying factor of ∼0.015 before the flow becomes stable. In Limit 3 when the horizontal effects of turbulence are included, the mean of $\Theta_c$ is 21.1 with a range from ∼10.5 to 52.3. Stability is attained with an increase in $\varepsilon$ by a factor of 21.1, which corresponds to a reduction in $Re_V$ by multiplying factor of ∼0.05, accompanied by a reduction in the 'horizontal' Reynolds number, $Re_H$, inversely proportional to $\varepsilon^{1/3} l^{4/3}$, by a multiplying factor of ∼0.36. (The wavelength of the fastest growing disturbance, $l$, varies little in the three limits, § 6.1, nor therefore with $\varepsilon$.)

### 6.3. *Hydraulics: the long waves*

Although the currents at the site near the sill in the Clyde Sea are non-parallel, the components transverse to an adopted direction normal to the ridge crest play no part in the determination of the long-wave speeds nor of their size in relation to the flow extrema, $U_{min}$ and $U_{max}$; the results are representative of the unidirectional flows addressed in Bell's theorem. The speed and stability of long waves (set in the numerical calculations as $k = 0.001$ m$^{-1}$, a wavelength of ∼6.3 km or 108 times

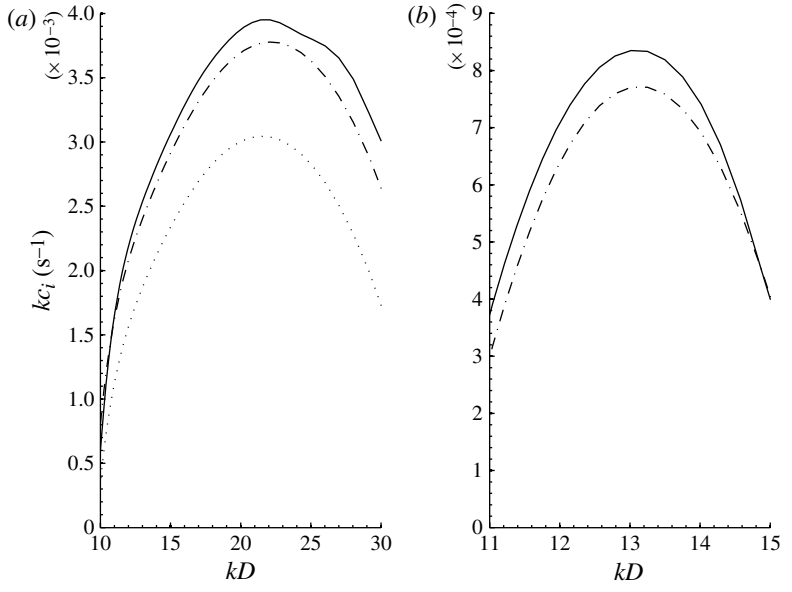


FIGURE 3. The growth rates, $kc_i$, of the most unstable mode versus $kD$, where $D = 58$ m is the water depth, at (*a*) Hr 16 and (*b*) Hr 10. The curves show: full line, Limit 1; dot-dashed line, Limit 2; dotted line, Limit 3. (Hr 10 is stable in Limit 3 so no curve is shown, and Hr 14 is stable with zero growth rates in all three limits; table 1.)

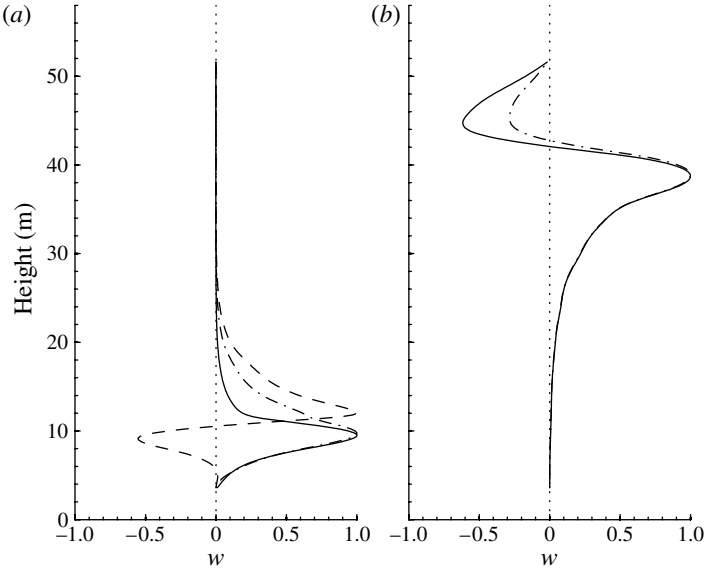


FIGURE 4. The profiles of vertical velocity, $w$, of the disturbance of maximum growth rates normalized to a maximum of unity at (*a*) Hr 16 and (*b*) Hr 10. The curves show: full line, Limit 1; dot-dashed line, Limit 2; dashed line, Limit 3. (Hr 10 is stable in Limit 3 so no curve is shown, and Hr 14 is stable with zero growth rates in all three limits; table 1.)

greater than the water depth of 58 m) are found by solution of the T–G equation in the three limits, taking the flows, $U_{50}(z)$, as the mean flow components in a direction away from the sill of 50° to the north shown in figure 1. Two solutions, each stable, are found for each of the first three modes, one travelling at a speed, $c_r$, greater than $U_{max}$ (denoted as $c_{+n}$, where $n$ is the mode number), the other ($c_{-n}$) with a speed less than $U_{min}$.

The minimum and maximum flow and the long-wave speeds for 24 hourly periods in the three limits are shown in figure 5. Figures 5(*a*), 5(*c*) and 5(*e*) show the speeds, $U_{min} - N_{max}D/\pi$, $U_{min}$, $c_{-n}$ for modes 1, 2 and 3 respectively, and figures 5(*b*), 5(*d*) and 5(*f*) the speeds $c_{+n}$, $U_{max}$ and $U_{max} + N_{max}D/\pi$, again for modes 1, 2 and 3 respectively, and each for the 24 hourly periods in Limits 1–3. Referring to this figure, it may be seen that:

(i) the speeds of the modes are ordered in accordance with Bell's theorem, i.e. $c_{-1} < c_{-2} < c_{-3}$ and $c_3 < c_2 < c_1$ (e.g. compare figures 5*b*, 5*d* and 5*f*, where the symbols approach the curve $U_{max}$ as the mode number increases);

(ii) the speeds, $c_{-n}$, in each mode $n$ generally increase with increased limit number (e.g. figure 5*a*), and $c_{+n}$ decrease (figure 5*b*). The exception is at Hr 19 for modes 1 and 2 (in figures 5*a* and 5*c*, respectively) when, for some unknown reason, the wave speeds, $c_{-n}$, in Limits 2 and 3 are less than in Limit 1;

(iii) in all three limits, the mode 1 speeds, $c_{-1}$ and $c_1$, are in $U_{min} - N_{max}D/\pi < c_{-1} < U_{min}$ or $U_{max} < c_1 < U_{max} + N_{max}D/\pi$. Moreover:

(iv) the flow is always subcritical to mode 1; for each limit there are mode-1 long waves that travel in both the positive (direction 050°) and negative direction, i.e. the speeds $c_{-n}$ are all negative and $c_{+n}$ are all positive. However:

(v) although all mode 2 and 3 waves lie within the ranges $U_{min} - N_{max}D/\pi < c_{-n}$ and $c_n < U_{max} + N_{max}D/\pi$,

(vi) some mode 2 and 3 waves lie within the range $U_{min}$ to $U_{max}$, e.g. $U_{min} < c_{-2}$ in Limit 3, figure 5(*c*), Hr 6, or $c_2 < U_{max}$ in Limit 2, figure 5(*d*), Hr 15. This is apparently contrary to Bell's theorem, but we recall that here $Ri_{min} < 1/4$;

(vii) at Hr 7, both long mode 2 wave speeds, $c_{-2}$ and $c_2$, are negative in all three limits, and at Hr 13, both are positive (figures 5*c* and 5*d*), supercritical conditions necessary for second mode hydraulic jumps. The same applies at these times for mode 3 (figures 5*e* and 5*f*): it therefore appears possible that the increase in phase speed of the $c_{-2}$ and $c_{-3}$ waves at Hr 14 (figure 5*c*) when $c_2$ and $c_3$ are both positive (figure 5*d*) transforms a subcritical mode 2 and 3 state into a supercritical modes 2 and 3 state;

(viii) in some cases (e.g. in mode 3 at Hr 0, figures 5*e* and 5*f*, where $c_{-1} < 0$ and $c_1 > 0$, but $c_{-2}$, $c_{-3}$, $c_2$ and $c_3$ are all positive) the flow is subcritical at Limit 1 but supercritical in Limits 2 and 3. Here the effect of turbulence is to change the critical state of the flow. (Although fairly large and abrupt – within an hour – changes in the depth of isotherms occur during the 24 h record, none can definitely be identified as being associated with hydraulic jumps. Further observations are required.)

With reference to (vi) above, although the majority of speeds calculated in Limit 1 by Gregg & Pratt (2010) also lie outside the range, similar 'entry' into the range $U_{min}$ to $U_{max}$ is sometimes found for the modes 2 and 3 even when $Ri_{min} > 1/4$ and may be a consequence of resolution, the solutions being based on a set of discrete measured values in $z$. In addition, concentration of oscillations in the eigenfunctions near the

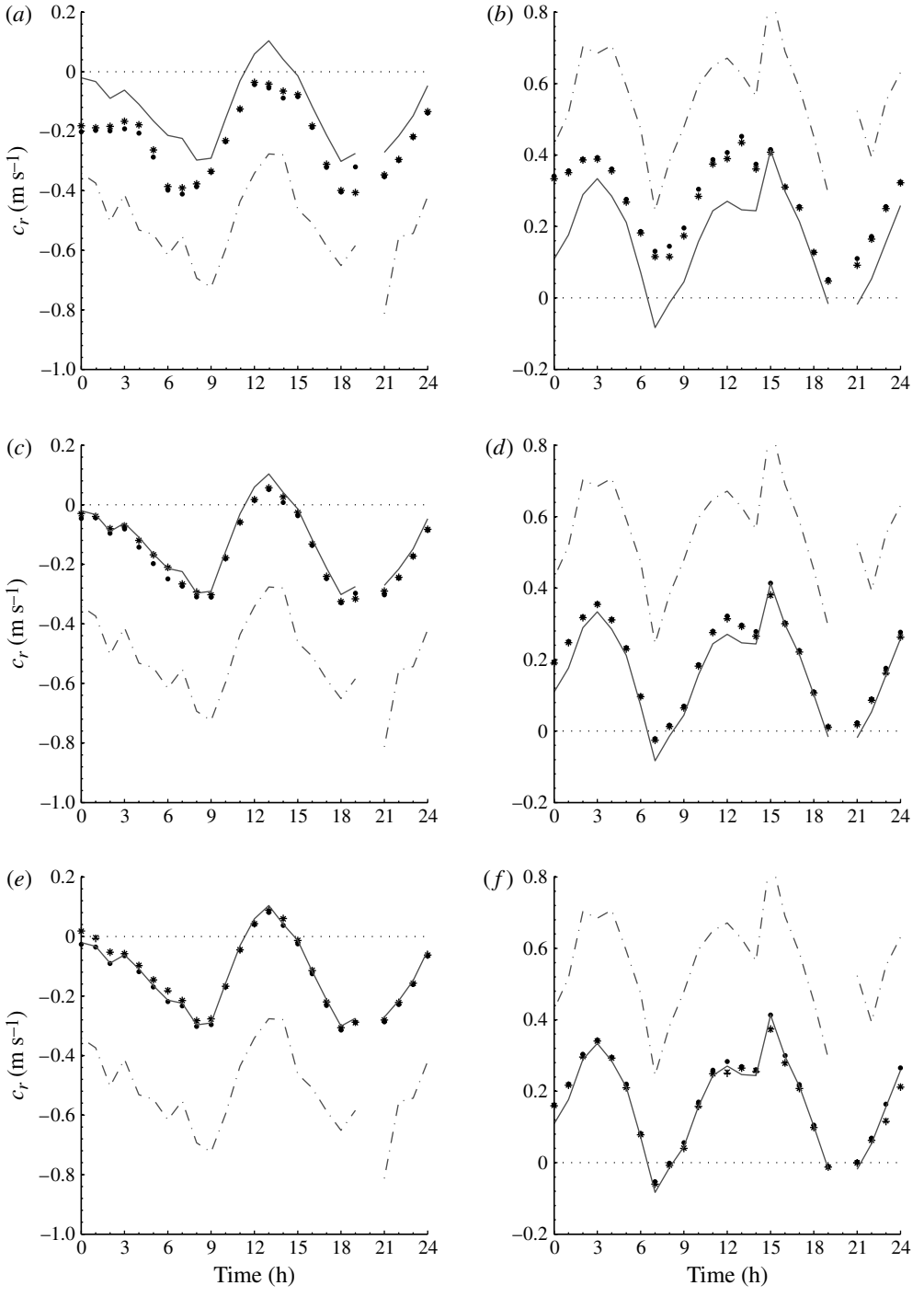


FIGURE 5. (*a*,*c*,*e*). The speeds $U_{min} - N_{max}D/\pi$ (dot-dashed lines), $U_{min}$ (full lines) and $c_{-n}$ (symbols) for modes (*a*) $n = 1$, (*c*) 2 and (*e*) 3, for the 24 hourly periods. (*b*,*d*,*f*): the speeds $U_{max} + N_{max}D/\pi$ (dot-dashed lines), $U_{max}$ (full lines) and $c_n$ (symbols) for modes (*b*) $n = 1$, (*d*) 2 and (*f*) 3, for the 24 hourly periods. The symbols represent the long-wave speeds, $c_n$ or $c_{-n}$ as •, Limit 1; ×, Limit 2 and +, Limit 3. Zero velocity is marked by the horizontal dotted lines.

levels where $U = U_{min}$ or $U_{max}$, makes ascribing the mode number uncertain (Pratt, private communication, 2011). The same is true here; the ordering of the modes by zero crossing sometimes leads to ambiguity: in the numerical solutions, there may be more than one mode with the same number of zero-crossing points.

## 7. Discussion and summary

The effect of turbulence on the stability and hydraulic state of stratified shear flows is examined, making several assumptions about the nature and representation of turbulence. Coefficients of eddy viscosity and diffusivity are used, expressed in terms of quantities that can be measured in the ocean, including the rate of dissipation of turbulent kinetic energy per unit mass, $\varepsilon$. Expressions for the horizontal coefficients, supposed independent of horizontal direction, are adopted following the discussion in § 3.2, expressions at present untested by observations.

With these and other assumptions, the effects of turbulence on flow stability are assessed by applying the analysis to data from the Clyde Sea. Smaller values of $Ri$ than predicted using the inviscid and non-diffusive T–G equation are required to produce instability when the effects of turbulence are included (§ 6.1). Flows that are stable in Limit 1, neglecting turbulent viscosity or diffusivity, become more so ($Ri_{min}$ becomes even greater than $Ri_c$) in Limits 2 and 3 when turbulence is included. It is concluded that the main effect of turbulence on the stability of the observed flows is a reduction of the growth rates of small disturbances. The effect of vertical transfers of momentum and density represented by $A_V$ and $K_V$ are, however, relatively small; the effects of the horizontal transfers, represented by the coefficients, $A_H$ and $K_H$, are generally much greater. Adding the vertical coefficients (Limit 2) reduces the growth rate, $(kc_i)_{max}$, by an average of 4.9 %, increases $\Phi_c$ by ∼5.7 % and reduces the critical Richardson number, $Ri_c$, found by imposing a variation $(1 + \Phi_c)$ on the flow, by 5.5 %. At Limit 3 the three measures, $(kc_i)_{max}$, $\Phi_c$ and $Ri_c$ are reduced from the Limit 1 values by 19.0 %, 22.7 % and 16.2 %, respectively. Some flows that are unstable in the absence of the effects of turbulence are stabilized: at Hr 11, for example, turbulence is sufficient to stabilize the flow that, in Limit 1, is unstable.

No cases are found in the data set from the Clyde Sea in which the critical Richardson number of turbulent stratified shear flows exceeds 1/4; the Miles–Howard theorem, valid when viscous and diffusive effects are negligible, appears to continue to be valid when the effects of turbulent transfers of momentum and mass are represented by eddy coefficients.

The mean values of $\Phi_c$ and $\Theta_c$ for the turbulent flows in the Clyde Sea provide measures of the marginality of the observed flows, their proximity to neutral conditions. Since $Ri_{min} = Ri_c\,(1 + \Phi_c)^2$, with $\Phi_c = -0.316$ in Limit 2 (§ 6.1), typical values of $Ri_{min}$ would have to be increased by a factor of 2.14 to bring the flow to stability at $Ri_{min} = Ri_c$. The equivalent factor is 1.82 in Limit 3. In contrast when $\varepsilon$ is varied (§ 6.2), $\Theta_c = O(65)$ in Limit 2; the mean 'vertical' Reynolds number of the flow, $Re_V$, must be reduced by a multiplying factor of ∼0.015 for unstable flows to be made stable at some value, say $Re_{V_c}$. In Limit 3 the corresponding factors are 0.05 and 0.36 for $Re_V$ and $Re_H$, respectively. In this sense in the $Ri$, $Re_V$, $Re_H$ space (where $Ri_c$, $Re_{V_c}$, $Re_{H_c}$ determines the surface of neutral stability), the unstable flows are relatively further from neutral stability in Reynolds number, $Re_V$, than in Richardson number.

We might, however, envisage a flow with moderate or small rates of dissipation becoming unstable, resulting in enhanced turbulence that increases $\varepsilon$ and stabilizes the flow. The following collapse of turbulence and reduction in $\varepsilon$ would lead to the

flow again becoming unstable, repeating the cycle, and thus maintaining conditions in a state of marginal stability. Whilst such a cycle is perhaps plausible, the discussion does not account for any changes produced in the velocity and density by turbulent mixing nor, in the natural environment, for the effects of other processes, such as internal waves perhaps radiating from an unstable region. (The envisaged repetition is not unlike that observed in a tilted tube filled with two layers of different density reported by Mittendorf 1961; see also Turner 1973, § 5.3.2, the flows in that case accelerating up and down slope, becoming unstable to Kelvin–Helmholtz instability, the turbulent Reynolds stresses transferring momentum across the tube and so reducing and restabilizing the flow, that again accelerates under the component of gravity parallel to the tube. Mittendorf observed this cycle to repeat up to three times. This repetition is discussed by Thorpe & Ozen 2007, in considering the possibly marginal conditions of winter cascading flows down the sloping sides of Lake Geneva.)

We can compare the order of magnitude of the viscous terms $\nabla_H \cdot (A_H \nabla_H \boldsymbol{u})$ and $\partial/\partial z(A_V \partial u/\partial z)$ (or those in $w$) in the linearized version of (2.1) and of the diffusive terms $\nabla_H \cdot (K_H \nabla_H b')$ and $\partial/\partial z(K_V \partial b'/\partial z)$ in the linearized (2.3). The ratio of the magnitude of the viscous terms is $(A_H/A_V)\,(l_{A_z}/l)^2$, supposing that the vertical scale $l_{A_z}$ characterizes the length scale over which vertical gradients of the eddy coefficient, $A_V$, and $u$ (or $w$) occur, while $l$ is the corresponding scale of the horizontal variation of $u$ (or $w$). Now $A_H/A_V = (2.9 \pm 0.8) \times 10^{-2} \varepsilon^{1/3} l^{4/3}/(0.2\varepsilon/N^2) = (1.45 \pm 0.4) \times 10^{-1}\,(l/L_{O_z})^{4/3}$ after using $L_{O_z} = \varepsilon^{1/2} N^{-3/2}$, and so the ratio is equal to $(1.45 \pm 0.4) \times 10^{-1}\,(l/L_{O_z})^{4/3}\,(l_{A_z}/l)^2$. Similarly, supposing that a scale $l_{K_z}$ characterises the length scale over which vertical gradients of the eddy coefficients and $b'$ occur, while $l$ is the corresponding horizontal scale of variation of $b'$, we find the ratio of diffusion terms in (2.3) to be approximately $(1.45 \pm 0.4) \times 10^{-1}\,(l/L_{O_z})^{4/3}\,(l_{K_z}/l)^2$. With typical values for the scale of the fastest growing disturbances, $l \sim 20$ m, and $l_{A_z} = l_{K_z} \sim 5$ m and $L_{O_z} \sim 0.1$ m (see figure 2), the ratio of each of the pairs of terms is $\sim$10; horizontal viscosity dominates the contribution to the growth rates of the velocity, $u$ (or $w$) in (2.1), and horizontal diffusivity dominates the contribution to the growth rates of the buoyancy, $b'$ in (2.3). This is quantitatively consistent with their effects on the largest growth rates of small disturbances.

However the estimation of the constant $C$ in (3.4) that determines the constant in the formulation, (3.6), for the horizontal eddy coefficients requires further consideration. Okubo's (1971) data for $K_D$ as a function of scale, $l$, from $l \sim 1$ km down to $\sim$20 m are fitted by (3.5), but no estimates of the relation are available at smaller $l$. The constant, $C$, in (3.4) (i.e. $K_D = C\varepsilon^{1/3} l^{4/3}$) is found by equating the expressions (3.4) and (3.5) for $K_D$, taking a mean observed value of $\varepsilon$. Assuming $K_H = K_D$ then leads to an expression for $K_H$. But if there is an input of energy, e.g. from breaking internal waves, at scales less than 20 m that leads to an augmentation of the dissipation rate, the value of $\varepsilon$ appropriate in (3.4) at scales of 20 m will be less than the mean value at the small scales measured by the FLY microstructure probe, and so $C$ will be underestimated. The ratio, $l_*/L_{O_z}$, is about 4 when $K_V = K_H$ (see § 3.2), and will therefore be too large. The values of $A_H$ and $K_H$ appropriate at the scales of $\sim$20 m of the fastest growing disturbances should, however, be increased by increasing $C$ but proportionally reduced by decreasing $\varepsilon$ in (3.6) to its value at 20 m scales; the net effect on the eddy coefficients may be slight. Further information is required about horizontal dispersion at scales $<$20 m and $\sim A_H$ and $K_H$ to improve the present tentative formulation of the horizontal effects of turbulence.

Turbulence reduces the range of long-wave speeds in both directions, i.e. for each mode, $n$, the speed, $c_{-n}$, of the fastest negatively propagating long wave generally

increases when the effects of turbulence are introduced, while the corresponding positive $c_{+n}$ speed decreases (§ 6.3). Although the wave speeds generally fall within the bounds defined by Bell's theorem, a subcritical flow may become supercritical as a consequence of the presence of turbulence: the presence of turbulence may change the hydraulic state of a stratified shear flow.

At the site in the Clyde Sea, the turbulent state of the observed flow appears, however, to have generally a relatively small effect on its stability or on the hydraulic conditions. Whilst there the neglect of turbulent effects may consequently be justified, it is not so in general: studies made of the stability of flow in the Equatorial Pacific show a much greater influence of turbulence.

## Acknowledgements

Dr T. Rippeth kindly allowed access to the Clyde Sea data (provided from NERC Grant NE/F002432) and we are grateful for his permission to use them. Very helpful advice and suggestions were provided by Dr M. Gregg. Z.L. was supported by the National Natural Science Foundation of China (Nos. 41006017 and 41076001) and the Fundamental Research Funds for the Central Universities (No. 2010121031). W.D.S. was supported by a Kirby Liang Fellowship at Bangor University and by the US National Science Foundation (No. 1030772).

## Appendix. The minimum Richardson number and extended Miles–Howard theorem

The Miles–Howard theorem, providing conditions for stable flow in terms of the magnitude of a minimum of the Richardson number, $Ri = N^2/(\mathrm{d}U/\mathrm{d}z)^2$, may be derived from the T–G equation found by combining (2.14) and (2.15) in Limit 1 using the method described by Howard (1961). Here $U$ is the velocity component of the mean flow in the direction, say $\phi$, of the disturbance relative to north. Flow components normal to the direction, $\phi$, do not appear in the governing equations. The minimum Richardson number, $Ri$, varies with $\phi$, and if its minimum exceeds 1/4 then, by the Miles–Howard theorem, disturbances in this flow direction are stable.

We suppose that the mean horizontal flow direction varies in $z$ and, at level $z$, the flow speed is $U_*$ in direction $\alpha$. Then the velocity component of the mean flow in the direction $\phi$ is $U = U_* \cos(\phi - \alpha) = U_*(\cos\phi\cos\alpha + \sin\phi\sin\alpha) = U_N\cos\phi + U_E\sin\phi$, where $U_E$ and $U_N$ are, respectively, the east and north components of $U_*$. Hence $\mathrm{d}U/\mathrm{d}z = \mathrm{d}U_N/\mathrm{d}z\cos\phi + \mathrm{d}U_E/\mathrm{d}z\sin\phi$, which (e.g. by differentiation with respect to $\phi$) has a maximum value, $S = [(\mathrm{d}U_E/\mathrm{d}z)^2 + (\mathrm{d}U_N/\mathrm{d}z)^2]^{1/2}$, when $\phi = \tan^{-1}[(\mathrm{d}U_N/\mathrm{d}z)/(\mathrm{d}U_E/\mathrm{d}z)]$ (which, since it varies in $z$, is not identified as the direction of the fastest growing disturbance). The minimum Richardson number at level $z$, as $\phi$ is varied, is therefore $N^2/[(\mathrm{d}U_E/\mathrm{d}z)^2 + (\mathrm{d}U_N/\mathrm{d}z)^2]$. This is the Richardson number plotted in the left column of figure 2.

It follows that an extension to the Miles–Howard theorem is that a horizontal, steady, inviscid and non-diffusive flow with components $(U(z), V(z))$, stably stratified with buoyancy frequency, $N(z)$, where $z$ is the upward vertical coordinate, is stable to small disturbances provided that $Ri = N^2/[(\mathrm{d}U/\mathrm{d}z)^2 + (\mathrm{d}V/\mathrm{d}z)^2]$ exceeds 1/4 everywhere in the flow (i.e. at all $z$). Sun *et al.* (1998, in their Appendix B) come to the same conclusion.

## REFERENCES


ASHFORD, O. M. 1985 *Prophet or Professor? The Life and Work of Lewis Fry Richardson*. Adam Hilger.

BAINES, P. G. 1995 *Topographic Effects in Stratified Flows*. Cambridge University Press.

BAINES, P. G. & MITSUDERA, H. 1994 On the mechanism of shear flow instabilities. *J. Fluid Mech.* **276**, 327–342.

BELL, T. H. 1974 Effects of shear on the properties of internal gravity waves. *Deutsche Hydrograph. Z.* **27**, 57–62.

DRAZIN, P. G. & REID, W. H. 1981 *Hydrodynamic Stability*. Cambridge University Press.

GAGE, K. S. 1971 The effect of stable thermal stratification on the stability of viscous parallel flows. *J. Fluid Mech.* **47**, 1–20.

GALPERIN, B., SUKORIANSKY, S. & ANDERSON, P. S. 2007 On the critical Richardson number in stably stratified turbulence. *Atmos. Sci. Lett.* **8**, 65–69.

GARGETT, A. E., OSBORN, T. R. & NASMYTH, P. W. 1984 Local isotropy and the decay of turbulence in a stratified fluid. *J. Fluid Mech.* **144**, 231–280.

GREGG, M. C. & PRATT, L. J. 2010 Flow and hydraulics near the sill of Hood Canal, a strongly sheared, continuously stratified fjord. *J. Phys. Oceanogr.* **40**, 1087–1105.

HOGG, A. M., WINTERS, K. B. & IVEY, G. N. 2001 Linear internal waves and the control of stratified exchange flows. *J. Fluid Mech.* **447**, 357–375.

HOWARD, L. N. 1961 Note on a paper by John W. Miles. *J. Fluid Mech.* **10**, 509–512.

KANTHA, L. H. & CLAYSON, C. A. 2000 *Numerical Models of Oceans and Oceanic Processes*. Academic.

KOPPEL, D. 1964 On the stability of flow of a thermally stratified fluid under the action of gravity. *J. Math. Phys.* **5**, 963–982.

LEDWELL, J. R., WATSON, A. J. & LAW, C. S. 1998 Mixing of a tracer in the pycnocline. *J. Geophys. Res.* **103** (21), 499–21, 529.

LIU, Z. 2010 Instability of baroclinic tidal flow in a stratified fjord. *J. Phys. Oceanogr.* **40**, 139–154.

MASLOWE, S. A. & THOMPSON, J. M. 1971 Stability of a stratified free shear layer. *Phys. Fluids* **14**, 453–458.

MILES, J. W. 1961 On the stability of heterogeneous shear flows. *J. Fluid Mech.* **10**, 496–508.

MITTENDORF, G. H. 1961 The instability of stratified flow. MSc thesis. State University of Iowa.

OKUBO, A. 1971 Oceanic diffusion diagrams. *Deep-Sea Res.* **18**, 789–802.

OLLITRAULT, M., GABILLET, C. & DE VERDIERE, A. C. 2005 Open ocean regimes of relative dispersion. *J. Fluid Mech.* **533**, 381–407.

OSBORN, T. R. 1980 Estimates of the local rate of vertical diffusion from dissipation measurements. *J. Phys. Oceanogr.* **10**, 83–89.

PRATT, L. J., DEESE, H. E., MURRAY, S. P. & JOHNS, W. 2000 Continuous dynamical modes in straits having arbitrary cross sections. *J. Phys. Oceanogr.* **30**, 2515–2534.

RICHARDSON, L. F. 1952 Transforms for the eddy-diffusion of clusters. *Proc. R. Soc. Lond.* A **214**, 1–20.

SHIH, L. H., KOSEFF, J. R., IVEY, G. N. & FERZIGER, J. H. 2005 Parameterization of turbulent fluxes and scales using homogeneous sheared stably stratified turbulence simulations. *J. Fluid Mech.* **525**, 193–214.

SMYTH, W. D., MOUM, J. N. & CALDWELL, D. R. 2001 The efficiency of mixing in turbulent patches: inferences from direct simulations and microstructure observations. *J. Phys. Oceanogr.* **31**, 1969–1992.

SMYTH, W. D., MOUM, J. N. & NASH, J. D. 2011 Narrowband, high-frequency oscillations at the equator. Part II. Properties of shear instabilities. *J. Phys. Oceanogr.* **41**, 412–428.

SUN, C., SMYTH, W. & MOUM, J. 1998 Dynamic instability of stratified shear flow in the upper equatorial Pacific. *J. Geophys. Res.* **103**, 10323–10337.

SUNDERMEYER, M. A. & LEDWELL, J. R. 2001 Lateral dispersion over the continental shelf: analysis of dye release experiments. *J. Geophys. Res.* **106**, 9603–9621.

SUNDERMEYER, M. A., LEDWELL, J. R., OAKEY, N. S. & GREENAN, B. J. W. 2005 Stirring by small-scale vortices caused by patchy mixing. *J. Phys. Oceanogr.* **35**, 1245–1262.

TAYLOR, G. I. 1935 Statistical theory of turbulence. *Proc. R. Soc. Lond.* A **151**, 421–478.

THORPE, S. A. 1969 Neutral eigensolutions of the stability equations for stratified shear flow. *J. Fluid Mech.* **36**, 673–683.

THORPE, S. A. 1971 Experiments on the instability of stratified shear flows: miscible fluids. *J. Fluid Mech.* **46**, 299–319.

THORPE, S. A. 2005 *The Turbulent Ocean*. Cambridge University Press.

THORPE, S. A. 2010 Turbulent hydraulic jumps in a stratified shear flow. *J. Fluid Mech.* **654**, 305–350.

THORPE, S. A. & HALL, A. J. 1977 Mixing in upper layer of a lake during heating cycle. *Nature* **265**, 719–722.

THORPE, S. A. & LIU, Z. 2009 Marginal stability? *J. Phys. Oceanogr.* **39**, 2373–2381.

THORPE, S. A. & OZEN, B. 2007 Are cascading flows stable? *J. Fluid Mech.* **589**, 411–432, (and Corrigendum **631**, 2009, 441–442).

TURNER, J. S. 1973 *Buoyancy Effects in Fluids*. Cambridge University Press.

YIH, C.-S. 1955 Stability of two-dimensional parallel flows for three-dimensional disturbances. *Q. Appl. Maths* **12**, 434–435.

ZIKA, J. 2008 The stability of boundary layer flow. 2007 Program of Study: Boundary Layers, WHOI GFD Summer School 2007 *Tech. Rep.* WHOI-2008-05, pp. 143–170.

ZILITINKEVICH, S. S., ELPERIN, T., KLEEORIN, T., ROGACHEVSKII, I., ESQU, I., MAURITSEN, T. & MILES, M. W. 2008 Turbulence energetics in stably stratified geophysical flows: strong and weak mixing regimes. *Q. J. R. Meteorol. Soc.* **134**, 793–799.